Journal of The Electrochemical Society, **156** (11) B1354-B1360 (2009)
0013-4651/2009/156(11)/B1354/7/$25.00 © The Electrochemical Society

Carbon-Supported Pt–TiO_2 as a Methanol-Tolerant Oxygen-Reduction Catalyst for DMFCs

G. Selvarani,[a,*] S. Maheswari,[a] P. Sridhar,[a,,z] S. Pitchumani,[a] and A. K. Shukla[b,**,z]**

[a]*Central Electrochemical Research Institute-Madras Unit, Council of Scientific and Industrial Research, Madras Complex, Chennai 600 113, India*
[b]*Solid State and Structural Chemistry Unit, Indian Institute of Science, Bangalore 560 012, India*

Carbon-supported Pt–TiO_2 (Pt–TiO_2/C) catalysts with varying at. wt ratios of Pt to Ti, namely, 1:1, 2:1, and 3:1, are prepared by the sol–gel method. The electrocatalytic activity of the catalysts toward oxygen reduction reaction (ORR), both in the presence and absence of methanol, is evaluated for application in direct methanol fuel cells (DMFCs). The optimum at. wt ratio of Pt to Ti in Pt–TiO_2/C is established by fuel cell polarization, linear sweep voltammetry, and cyclic voltammetry studies. Pt–TiO_2/C heat-treated at 750°C with Pt and Ti in an at. wt ratio of 2:1 shows enhanced methanol tolerance, while maintaining high catalytic activity toward ORR. The DMFC with a Pt–TiO_2/C cathode catalyst exhibits an enhanced peak power density of 180 mW/cm^2 in contrast to the 80 mW/cm^2 achieved from the DMFC with carbon-supported Pt catalyst while operating under identical conditions. Complementary data on the influence of TiO_2 on the crystallinity of Pt, surface morphology, and particle size, surface oxidation states of individual constituents, and bulk and surface compositions are also obtained by powder X-ray diffraction, scanning and transmission electron microscopy, X-ray photoelectron spectroscopy, energy dispersive analysis by X-ray, and inductively coupled plasma optical emission spectrometry.
 [DOI: 10.1149/1.3223911]

Manuscript submitted May 14, 2009; revised manuscript received August 14, 2009. Published September 25, 2009.

Direct methanol fuel cells (DMFCs) have reached a high level of development and are now almost universally referred to as the sixth fuel cell type. In applications, they are set to function as power sources for a range of mobile applications, a situation brought about by the convenience of the storage of liquid fuels. For the expansion of the applications of DMFCs, efforts are being expended to develop improved electrocatalysts for the anode and for the cathode where methanol tolerance is preferred.[1]

In the literature,[2] four classes of oxygen-reduction catalysts have been employed with the DMFCs, namely, (*i*) noble metal catalysts, such as platinum, which when dispersed in particulate form on carbon exhibit high activity for oxygen reduction (however, these catalysts show little methanol tolerance); (*ii*) macrocyclic derivatives of transition-metal compounds, such as Co and Fe porphyrins, phthalocyanines, and tetraazaannulenes, which yield low current densities because of their relatively poor activity toward oxygen reduction reaction (ORR) (furthermore, their dispersion on high surface area substrates needs to be ameliorated); (*iii*) metallic oxides, particularly of the second and third row transition metals, which are not acid stable; and (*iv*) transition-metal compounds with other nonmetallic counterions derived from the chalcogenides, such as RuSe, which are active toward ORR but not with methanol oxidation, allowing them to be used in DMFCs even when methanol permeation takes place from the anode to the cathode. However, oxygen reduction activities of chalcogenide-based catalysts are much lower than that of Pt. Because of the above reasons, methanol-tolerant Pt-based catalysts are preferred in DMFCs for prolonged operations.

It is also reported that the addition of a base metal, such as iron, cobalt, nickel, and chromium, to platinum improves its methanol tolerance toward oxygen reduction at the cathode.[3-7] However, the alloy catalysts exhibit poor long-term stability due to the dissolution of the base metal. Recently, the introduction of a second platinum-group metal (PGM), such as palladium and gold, to platinum has found considerable attention due to their high oxygen reduction activity, methanol tolerance, and better durability.[8-12] However, the use of Pt-PGM alloys is cost intensive. Recently, stable metal oxides, such as Pt–MO_x (M = Ru, W, or Ti), have also been investigated for ORR and have been found to exhibit higher activity than Pt.[12-24] Among these Pt–TiO_2 catalysts, being cost effective and acid stable are particularly attractive. Brewer and Wengert[25] reported that the hypo d-electron character of titanium oxide facilitates its interaction with noble metals, like Pt, changing the catalytic activity of the noble metal. The change in the catalytic activity is explained using Hammer and Norskov's concept,[26] according to which the reactivity alters through the changes in the adsorbate interaction energy due to the shift in the local d-band position relative to the Fermi level. In the literature,[16-24] the suitability of TiO_2 as a catalyst support material has been studied extensively. Although TiO_2 shows higher durability in relation to conventional carbon supports, its electronic conductivity is relatively lower, which results in increased ohmic resistance for the cell.[16-18] Recently, an electrocatalytic oxygen reduction on a carbon-supported Pt–TiO_2 in the presence of methanol is reported by Rajalakshimi et al.[19] and Xiong and Manthiram.[22] But these studies exclude (*i*) the effect of the Pt to Ti ratio to the catalyst and (*ii*) a systematic physical characterization of the catalyst in conjunction with electrochemistry; a study on the performance optimization of DMFC utilizing the catalyst is also lacking.

In the present study, a Pt–TiO_2 nanocomposite catalyst with varying Pt to Ti at. wt ratios, namely, 1:1, 2:1, and 3:1, was supported onto carbon. The optimum atomic ratio of Pt to Ti in the Pt–TiO_2 composite catalyst for ORR in DMFC was determined by cyclic voltammetry (CV) and linear sweep voltammetry (LSV) in conjunction with cell polarization studies. To understand the influence of TiO_2 on the crystallinity of Pt, mean particle size, surface oxidation states of individual constituents, surface morphology, and particle size and bulk and surface compositions were studied by powder X-ray diffraction (XRD), X-ray photoelectron spectroscopy (XPS), transmission electron microscopy (TEM), scanning electron microscopy, energy dispersive analysis by X-ray (EDAX), and inductively coupled plasma optical emission spectrometry (ICP-OES).

Experimental

Preparation of Pt–TiO_2/C composite catalyst.— A sol–gel route was adopted to prepare Pt–TiO_2 nanocomposite catalysts. The required amount of titanium isopropoxide (Aldrich) was diluted with isopropanol and made into a homogeneous solution by ultrasonication. To prepare titania sol, 10 μL of 0.5 M aqueous H_2SO_4 was added to the titanium isopropoxide solution and agitated for 1 h. Finally, the required quantity of carbon-supported Pt (40 wt % from Alfa Aesar) was added with continuous stirring. The resultant mixture was left for 24 h to form a gel, followed by heating at 80°C for 1 h to remove all volatile substances present in it. The resulting cake

* Electrochemical Society Student Member.
** Electrochemical Society Active Member.
z E-mail: psridhar55@gmail.com; akshukla2006@gmail.com

was pulverized and subjected to heat-treatment at 600, 750, and 900°C in a flowing mixture of 90% N_2-10% H_2 for 5 h and cooled to room temperature. For comparison, the commercial 40 wt % Pt/C (Alfa Aesar) was also subjected to heat-treatment under similar conditions.

In the following text, the Pt–TiO_2/C samples heated at 600, 750, and 900°C are represented as 600, 750, and 900 Pt–TiO_2/C, respectively. The carbon-supported platinum heat-treated at 750°C is represented as 750 Pt/C, and the as-received platinum catalyst is represented as Pt/C. The Pt–TiO_2/C samples with varying atomic ratios of Pt to Ti, namely, 3:1, 2:1, and 1:1, are denoted as Pt–TiO_2/C (3:1), Pt–TiO_2/C (2:1), and Pt–TiO_2/C (1:1), respectively, and the heat-treated samples are represented by the heat-treatment temperature followed by the sample representation; for example, Pt–TiO_2/C (2:1) heat-treated at 750°C is represented as 750 Pt–TiO_2/C (2:1).

Electrochemical characterization.— Half-cell mode.— To study the ORR activity and methanol-tolerance ability of Pt/C and various Pt–TiO_2/C catalysts, LSV and CV measurements were performed using a computer-controlled electrochemical analyzer (Autolab PGSTAT-30).

Glassy carbon (GC) disks (with a geometric area of 0.071 cm^2) were used as the working electrode substrate for the CV and LSV measurements. Before each test, the electrodes were polished with 0.06 μm alumina to obtain a mirrorlike finish followed by rinsing with triple-distilled water in an ultrasonic bath. A precalibrated saturated calomel electrode (SCE) and a Pt foil were used as the reference and counter electrodes, respectively, in the three-electrode configuration. All electrochemical experiments were carried out at room temperature (~25°C).

To prepare the working electrode, a suspension of the catalyst was obtained by adding 4 mg of the catalyst in 8 mL water mixed with 30 wt % Nafion solution (DuPont) followed by sonication for 30 min. The suspension was quantitatively transferred to the surface of the polished GC disk. The disk electrode was dried at room temperature. To clean/activate the electrode surface, the electrode was cycled between −0.25 and 0.8 V with respect to SCE at a sweep rate of 50 mV/s to obtain reproducible voltammograms. The LSV experiments were performed using a rotating disk electrode (RDE), both in the presence and absence of methanol in oxygen-saturated 0.5 M aqueous $HClO_4$. The LSV data were recorded in the cathodic sweep direction at 1 mV/s from 0.8 to −0.25 V vs SCE over a range of rotations (400–2400 rpm) at room temperature (~25°C). Similar experiments were performed for all the catalysts studied here.

Fuel cell studies.— Fabrication of MEAs. Membrane electrode assemblies (MEAs) were fabricated following the procedure described in Ref. 12. Both the anode and the cathode comprised a backing layer, a gas-diffusion layer, and a reaction (catalyst) layer. A Teflonized (15 wt %) carbon paper (Toray TGP-H-120) of 0.35 mm thickness was employed as the backing layer to these electrodes. To prepare the gas-diffusion layer, a Vulcan XC72R carbon was suspended in cyclohexane and agitated in an ultrasonic water bath for 30 min. A 15 wt % Teflon suspension was added under sonication. The desired quantity of the resultant slurry was transferred onto a Teflonized carbon paper and was sintered in an air oven at 350°C for 30 min.

To prepare the reaction layer, 2 mg_{Pt}/cm^2 of a Pt–Ru (1:1 atomic ratio) supported on carbon (Alfa Aesar) with 10 wt % Nafion was used as the anode, while 2 mg_{Pt}/cm^2 of the catalyst with 30 wt % Nafion was used as the cathode. To establish an effective contact between the catalyst layer and the polymer electrolyte, a thin layer of Nafion solution (5 wt %) diluted with isopropyl alcohol in the 1:1 ratio was spread onto the surface of each electrode. The MEAs were obtained by hot pressing the cathode and the anode on either side of a pretreated Nafion 117 membrane under a compaction pressure of 60 kg cm^{-2} at 130°C for 3 min. The test MEAs were prepared with all the catalysts in a similar manner.

Polarization studies. The MEAs were evaluated using a conventional 25 cm^2 fuel cell fixture with a parallel serpentine flow field machined on graphite plates (Schunk Kohlenstofftechnik GmbH, Germany). After equilibration, the single cells were tested at 70°C with 2 M aqueous methanol at a flow rate of 30 mL/min at the anode and with humidified oxygen at a flow rate of 0.5 L/min at the cathode at atmospheric pressure. The flow rate was kept at 1 L/min while using air in place of oxygen. Measurements on cell potential as a function of current density were conducted galvanostatically using a LCN100-36 electronic load procured from Bitrode Corporation.

Physical characterization.— Powder XRD patterns for the catalysts were obtained on a Philips X'Pert diffractometer using Cu Kα radiation (λ = 1.5406 Å) between 20 and 80° in reflection geometry in steps of 0.034°/min. The morphology of the samples was examined under a TCNAI 20 G2 transmission electron microscope (200 kV). For this purpose, the samples were suspended in isopropyl alcohol and casted by dropping the catalyst solution onto a carbon-coated copper grid followed by solvent evaporation in a vacuum at room temperature (~25°C).

The XPS for the catalysts was recorded on a MultiLab 2000 (Thermofisher Scientific, U.K.) X-ray photoelectron spectrometer fitted with a twin anode X-ray source using Mg Kα radiation (1253.6 eV). For recording the desired spectrum, the powder sample was pressed onto a conducting carbon tape pasted with the indium-coated stainless steel stubs. The sample stubs were initially kept in the preparatory chamber overnight at 10^{-9} mbar to desorb any volatile species and then introduced into the analysis chamber at 9.8 × 10^{-10} mbar to record the spectra. High resolution spectra averaged over five scans with a dwell time of 100 ms in steps of 0.02 eV were obtained for the catalyst samples at the pass energy of 20 eV in the constant analyzer energy mode. Experimental data were curve fitted with a Gaussian and Lorentzian mix product function after subtracting the Shirley background. The spin-orbit splitting and the doublet intensities were fixed as described in the literature.[27] Relative intensities for the surface species were estimated from the respective areas of the fitted peaks.

ICP-OES was used to analyze the bulk compositions of Pt/C and Pt to Ti in various Pt–TiO_2/C catalysts. For this purpose, the catalysts were dissolved in concentrated aqua regia followed by dilution with water to concentrations ranging between 1 and 50 ppm as desired for the analysis. The actual composition was determined from the calibration curves of known standards. The surface morphology for various Pt–TiO_2/C catalysts was studied using a JEOL JSM 5400 scanning electron microscope, and their surface atomic compositions were obtained using the energy dispersive X-ray analysis facility provided with it.

Results and Discussion

Electrochemical measurements are performed to evaluate the electrochemical activity of the catalysts toward ORR. The steady-state CV for Pt/C and Pt–TiO_2/C with varying Pt to Ti ratio in deaerated 0.5 M aqueous $HClO_4$ are presented in Fig. 1. In this study, all samples exhibit the features of the hydrogen adsorption/desorption region between −0.24 and 0.1 V (vs SCE) followed by the "double-layer" potential region; at potentials >0.45 V (vs SCE), oxide formation/desorption regions are observed. Electrochemical surface area (ESA) values for all samples are presented in Table I. The ESA value for Pt/C is higher than that for 750 Pt/C, which may be due to particle aggregation by heat-treatment.[21] The 750 Pt–TiO_2/C with varying Pt to Ti atomic ratio shows a higher ESA than the 750 Pt/C sample, which appears to be due to the increased surface area of smaller Pt particles induced by titanium oxide as revealed by TEM and powder XRD studies. However, the ESA values for 750 Pt/C and 750 Pt–TiO_2 are less than that for Pt/C, which is attributed to the increased particle size upon heat-treatment. Among the three catalysts, namely, 750 Pt–TiO_2/C (3:1), 750 Pt–TiO_2/C (2:1), and 750 Pt–TiO_2/C (1:1), 750 Pt–TiO_2/C (2:1) exhibits the highest ESA value. It is expected that the ESA for Pt would increase with increasing TiO_2 content in the catalyst due to decreasing size effect. However, the 750 Pt–TiO_2/C (1:1) catalyst

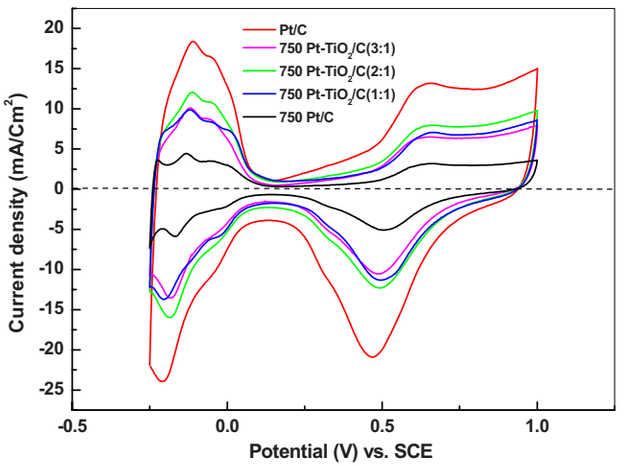

Figure 1. (Color online) Steady-state CVs for the Pt/C, 750 Pt/C, and 750 Pt–TiO_2/C with varying Pt to Ti atomic ratios in the N_2-saturated 0.5 M aqueous $HClO_4$ with a scan rate of 50 mV/s.

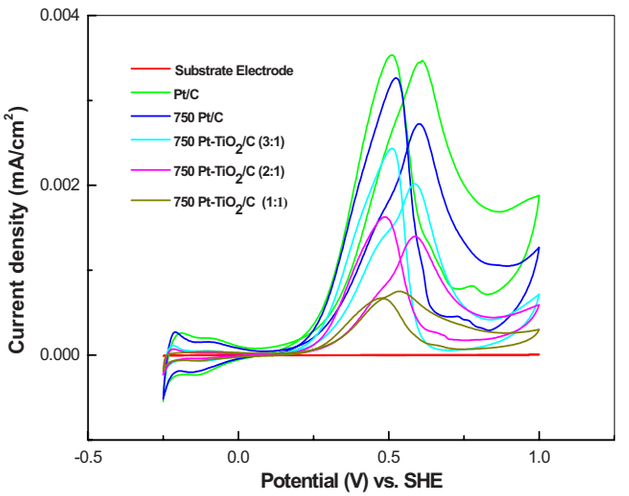

Figure 2. (Color online) CVs for the Pt/C and 750 Pt–TiO_2/C catalysts with varying Pt to Ti atomic ratios in the N_2-saturated 0.5 M $HClO_4$(aq) + 0.5 M CH_3OH(aq) solution with a scan rate of 50 mV/s.

provides a lesser ESA than 750 Pt–TiO_2/C (2:1) due to a larger quantity of TiO_2 that may encapsulate the Pt active sites.

Before the evaluation of 750 Pt–TiO_2/C catalysts for the DMFC cathode, the ability of the catalyst is assessed for methanol oxidation in half-cell mode. The methanol oxidation ability of Pt/C and 750 Pt–TiO_2/C with varying Pt to Ti atomic ratio, namely, 3:1, 2:1, and 1:1, is investigated by CV in a 0.1 M H_2SO_4 + 0.5 M CH_3OH solution, and the corresponding data are shown in Fig. 2; the CV for the bare GC electrode is also included. It is evident that the substrate has little catalytic activity for methanol oxidation. However, both Pt/C and 750 Pt–TiO_2/C with varying atomic ratio of Pt to Ti on a GC electrode show two oxidation peaks related to the oxidation of methanol and the corresponding intermediates produced during the methanol oxidation. The methanol oxidation currents for Pt/C and 750 Pt/C are higher in relation to the 750 Pt–TiO_2/C catalysts. Among the 750 Pt–TiO_2/C catalysts, 750 Pt–TiO_2/C (2:1) and 750 Pt–TiO_2/C (1:1) show a lesser methanol oxidation current in relation to 750 Pt–TiO_2/C (3:1). The methanol adsorption–dehydrogenation process requires at least three neighboring Pt atoms in the proper crystallographic arrangement.[28] Among the 750 Pt–TiO_2/C samples, the probability of finding three neighboring Pt atoms on the surface of 750 Pt–TiO_2/C (2:1) and 750 Pt–TiO_2/C (1:1) appears to be lower than that for Pt/C and 750 Pt–TiO_2/C (3:1). Accordingly, the methanol oxidation current happens to be low for 750 Pt–TiO_2/C (2:1) and 750 Pt–TiO_2/C (1:1) catalysts.

The catalysts have also been performance tested in DMFCs. The cell polarization data for the 750 Pt–TiO_2/C cathodes with varying Pt to Ti atomic ratios in a methanol/O_2 DMFC are compared with the DMFCs employing Pt/C and 750 Pt/C cathodes in Fig. 3. The DMFC with a 750 Pt–TiO_2/C (2:1) cathode performs better in relation to the DMFCs comprising 750 Pt–TiO_2/C (3:1), 750 Pt–TiO_2/C (1:1), and Pt/C cathodes. The DMFC comprising a 750 Pt–TiO_2/C (2:1) cathode shows an enhanced peak power density of 180 mW/cm^2 in relation to the peak power density of 80 mW/cm^2 for the DMFC with a Pt/C cathode at 70°C. Because the anode in all the DMFCs is identical, the enhanced performance for the DMFC with the 750 Pt–TiO_2/C (2:1) cathode is clearly due to the enhanced ORR with decreased methanol oxidation on the catalyst. These data corroborate the CV data presented in Fig. 1 and 2. The enhancement of electrocatalytic activity could be due to a change in the electronic structure of the catalyst arising from the electronic interactions between Pt and TiO_2 because of the hypo d-electron character of TiO_2 and the hyper d-electron character of Pt.[18] Although TiO_2 is a semiconducting oxide with a relatively high bandgap of ~3.2 eV, the wt % of TiO_2 in the optimized catalyst is only 6 wt %, and hence the effect of TiO_2 on the conductivity of the catalyst layer is expected to be negligibly small. The conductivity values for the two-phase mixtures may as well exceed the conductivity values of the pure constituents.[29-31] Accordingly, the electrical properties of TiO_2 are supposedly only ameliorating.

To examine the effect of heat-treatment temperature on the performance of the Pt–TiO_2 (2:1) catalyst, cell polarization studies were performed on samples heat-treated at varying temperatures, namely, 600, 750, and 900°C (Fig. 4). Among these samples, 750 Pt–TiO_2/C (2:1) exhibits the highest performance in relation to 600 Pt–TiO_2/C (2:1) and 900 Pt–TiO_2/C (2:1), which could be due to the balancing effect at higher temperatures between the increased electronic conductivity of TiO_2 [16] and the increase in Pt particle size. In the present study, 750 Pt–TiO_2/C (2:1) has the optimum performance. Because a practical DMFC uses oxygen from air as the oxidant, the performance data for DMFC operating with methanol and air at 30 and 70°C are presented in Fig. 5. The data show that there is a gain of 77 and 121 mV at 100 mA/cm^2 at 30 and 70°C for DMFCs comprising Pt–TiO_2/C and Pt/C as cathode catalysts, respectively. A durability study on the DMFC employing air as

Table I. Compositions and structural parameters for the Pt/C and Pt–TiO_2/C catalysts with varying Pt and Ti atomic ratios.

Catalyst	Particle size in TEM (nm)	Pt to Ti atomic ratio in ICP-OES (%)	Pt to Ti atomic ratio in EDAX (%)	ESA (m^2/g)
Pt/C	4	—	—	42.9
750 Pt/C	>20	—	—	14.5
750 Pt–TiO_2/C (3:1)	11	73.35:26.65	71.65:28.35	29.8
750 Pt–TiO_2/C (2:1)	9	64.42:35.58	66.25:33.75	38.3
750 Pt–TiO_2/C (1:1)	7	43.42:56.58	50.31:49.69	35.6

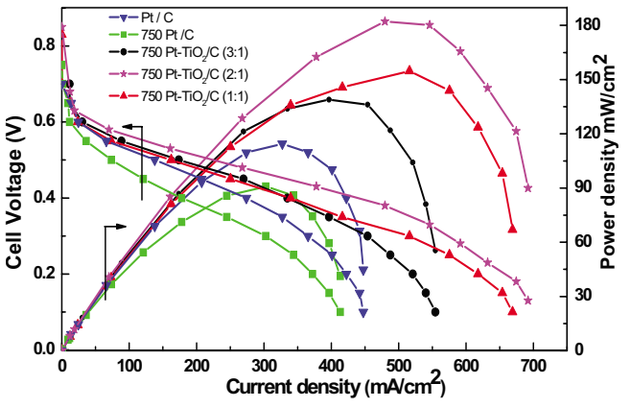

Figure 3. (Color online) Steady-state performance data of DMFCs (CH_3OH and O_2) for Pt/C, 750 Pt/C, and 750 Pt–TiO_2/C with varying Pt to Ti atomic ratios at 70°C.

the oxidant was also conducted to evaluate the stability of the catalyst, and the data are presented in Fig. 6. The DMFC sustains a load current density of 150 mA/cm^2 for 100 h.

To evaluate the influence of methanol on ORR, LSV experiments were performed using RDE to evaluate the electrocatalytic properties of Pt/C and 750 Pt–TiO_2/C (2:1) toward ORR in the presence and absence of methanol. The ORR data were obtained in the absence of methanol for 750 Pt–TiO_2/C (2:1) and Pt/C cathode at selected rotations, namely, 400, 800, 1200, 1600, 2000, and 2400 rpm (data not shown). For both Pt/C and 750 Pt–TiO_2/C (2:1) cathodes, the current densities (the current normalized to the geometric area of the electrode) are proportional to the rotation speed (ω) confirming ORR to be limited by the diffusion of oxygen. The ORR activity data for the Pt/C and 750 Pt–TiO_2/C (2:1) cathodes at 1200 rpm are shown in Fig. 7. The enhanced electrocatalytic activity for the Pt–TiO_2/C cathode can be explained by an electronic factor, namely, the change in the d-band vacancy in Pt in conjunction with the geometric effect.[28] Both effects may enhance the reaction rate for the oxygen adsorption and cleavage of the O–O bond during ORR. The diffusion current (i_d) values for both the Pt/C and 750 Pt–TiO_2/C (2:1) are almost similar, indicating that the ORR mechanism on both catalysts are similar.

The performance data for the 750 Pt–TiO_2/C (2:1) and Pt/C cathodes toward ORR in the presence of methanol are also presented in Fig. 7. The 750 Pt–TiO_2/C (2:1) cathode exhibits a higher ORR

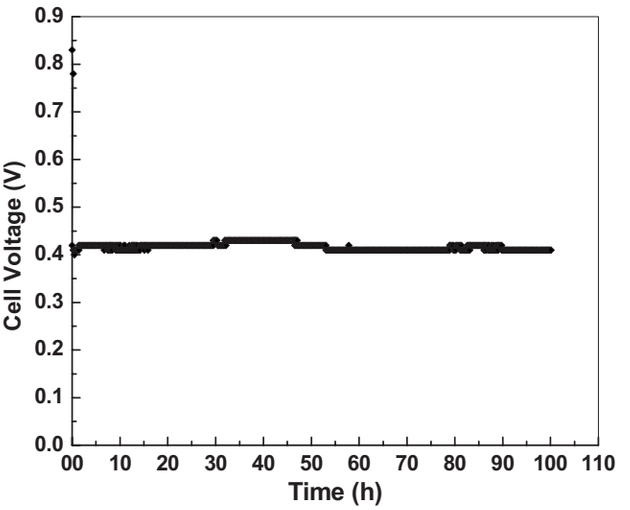

Figure 6. Durability data for DMFC (methanol/air) with a Pt–TiO_2/C (2:1) catalyst at a load current density of 150 mA/cm^2 at 70°C.

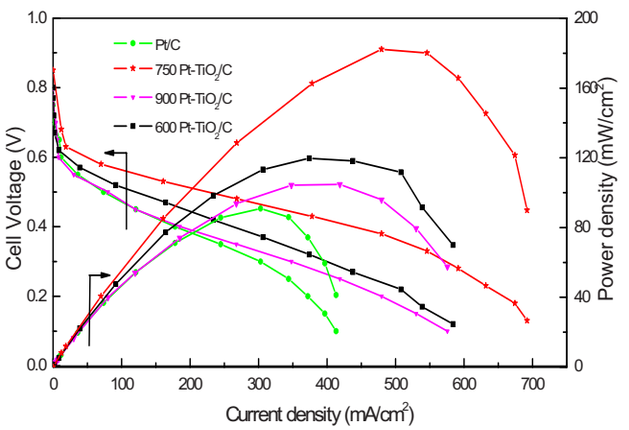

Figure 4. (Color online) Steady-state performance data of DMFCs (CH_3OH and O_2) for Pt/C, 600 Pt–TiO_2/C (2:1), 750 Pt–TiO_2/C (2:1), and 900 Pt–TiO_2/C (2:1) at 70°C.

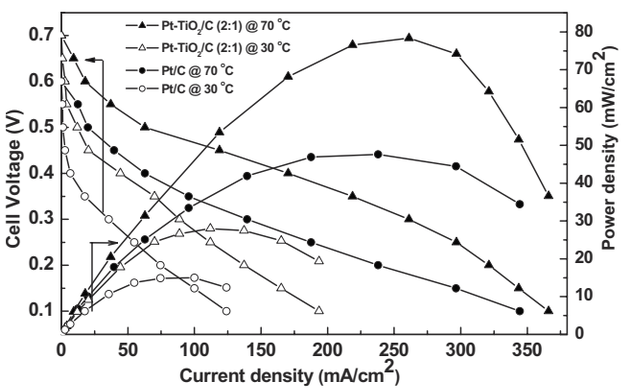

Figure 5. Steady-state performance data for DMFCs (methanol/air) with Pt/C and Pt–TiO_2/C (2:1) catalysts at 70 and 30°C.

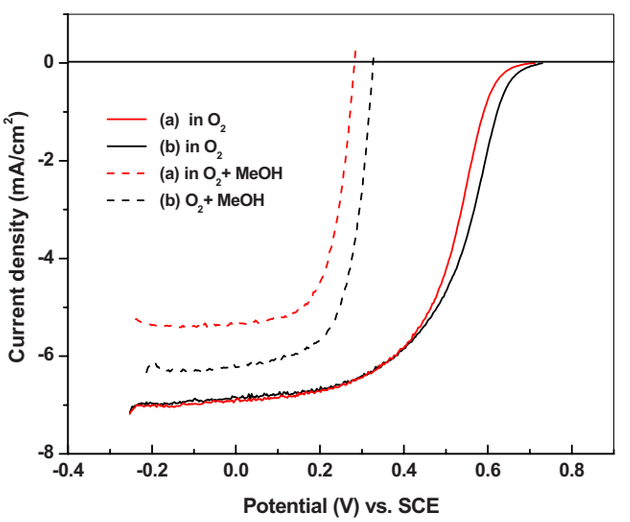

Figure 7. (Color online) LSV data for the ORR on the (a) 750 Pt/C and (b) 750 Pt–TiO_2/C (2:1) catalysts in O_2-saturated 0.5 M aqueous $HClO_4$ in the presence and absence of methanol at a 1 mV/s scan rate (rotation rate: 1200 rpm).

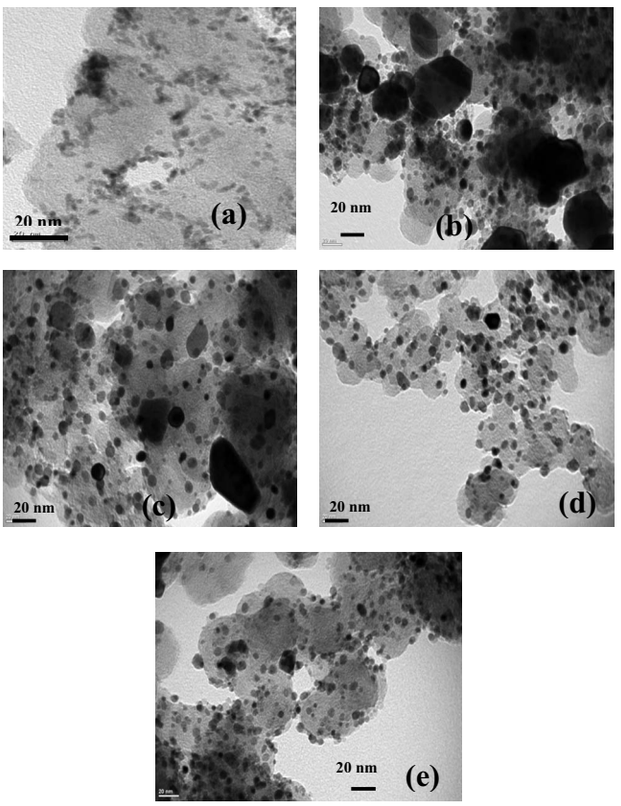

Figure 8. Transmission electron micrographs for the (a) Pt/C, (b) 750 Pt/C, (c) 750 Pt–TiO_2/C (3:1), (d) 750 Pt–TiO_2/C (2:1), and (e) 750 Pt–TiO_2/C (1:1) catalysts.

activity with minimum methanol oxidation. These data clearly indicate a higher overpotential for ORR at any current density in the presence of methanol for the Pt/C cathode in relation to the 750 Pt–TiO_2/C (2:1) cathode. The significant increase observed in the overpotential for ORR on the Pt/C and 750 Pt–TiO_2/C (2:1) cathodes in the presence of methanol reflects a competing oxygen reduction and methanol oxidation reactions. These studies confirm that the 750 Pt–TiO_2/C (2:1) cathode has a higher ORR selectivity and better methanol tolerance in relation to the Pt/C cathode.

The aforesaid electrochemical data confirm that the 750 Pt–TiO_2/C (2:1) cathode gives the optimum performance for DMFCs. To explore the reason for the higher performance observed in the 750 Pt–TiO_2/C (2:1) cathode in relation to the 750 Pt–TiO_2/C (1:1), 750 Pt–TiO_2/C (2:1), and Pt/C cathodes, the catalysts have been characterized by TEM, XRD, XPS, EDAX, and ICP-OES as discussed below.

Figure 8 depicts the TEM images for the as-received Pt/C, 750 Pt/C, and 750 Pt–TiO_2 catalysts with varying Pt to Ti atomic ratio. The Pt/C catalyst's nanoparticles with a narrow particle size distribution are well dispersed on the support. The particle size of Pt increased significantly after heat-treatment. These values agree with the CV data shown in Fig. 1. In the 750 Pt–TiO_2/C catalyst, the particle size of Pt decreases with an increasing ratio of Pt to Ti. This indicates that TiO_2 hinders the aggregation of particles. Amorphous titanium oxide is barely visible due to high platinum loading on the carbon. However, platinum is homogeneously dispersed on the carbon. In this study, the mean size of the metal nanoparticles on the carbon support is obtained by measuring 200 randomly chosen particles in the magnified TEM images (Table I).

To understand the influence of TiO_2 on the crystallinity of Pt in the catalysts, XRD patterns were obtained for the various catalysts studied here, but only the XRD patterns for Pt/C, 750 Pt/C, and 750 Pt–TiO_2/C (2:1) are included in Fig. 9 for the sake of brevity. The XRD patterns for both Pt/C and Pt–TiO_2/C show peaks corresponding to (111), (200), (220), (311), and (222) planes, which is characteristic of the face-centered cubic structure of Pt. The diffraction peaks of the 750 Pt/C catalyst are sharper than those of the Pt/C catalyst, indicating a larger particle size of the former due to Pt aggregation during heat-treatment; these data agree with CV data (Fig. 1). The positions of the Pt reflections do not exhibit any notable change in 750 Pt–TiO_2/C (2:1) compared to both the Pt/C and 750 Pt/C. Furthermore, no characteristic peaks corresponding to titanium oxide are observed in the pattern of the Pt–TiO_2/C (2:1) sample, suggesting that titanium oxide is finely divided or amorphous. The average size values of Pt particles in Pt/C, 750 Pt/C, and 750 Pt–TiO_2/C (2:1) are estimated from the broadening of Pt(111) peak by using the Scherrer equation $d = 0.94\lambda_{k\alpha1}/B_{(2\theta)} \cos \theta_B$ where d is the average particle diameter, $\lambda_{k\alpha1}$ is the wavelength of the X-ray radiation (1.5406 Å), θ_B is the Bragg angle for the (111) peak, and $B_{(2\theta)}$ is the full width at half-maximum (fwhm, in radian) of the diffraction peak. From the particle size data, the mean particle size for both the 750 Pt/C and 750 Pt–TiO_2/C (2:1) catalysts is larger than that of the Pt/C catalyst. The mean particle size of Pt crystallites in the 750 Pt–TiO_2/C (2:1) catalyst decreased due to TiO_2 in comparison to the 750 Pt/C catalyst. A judicious selection of preparatory conditions, in particular, the precursor, and composition of reactants and heat-treatment temperature is mandatory for synthesizing a finely divided Pt–TiO_2/C.

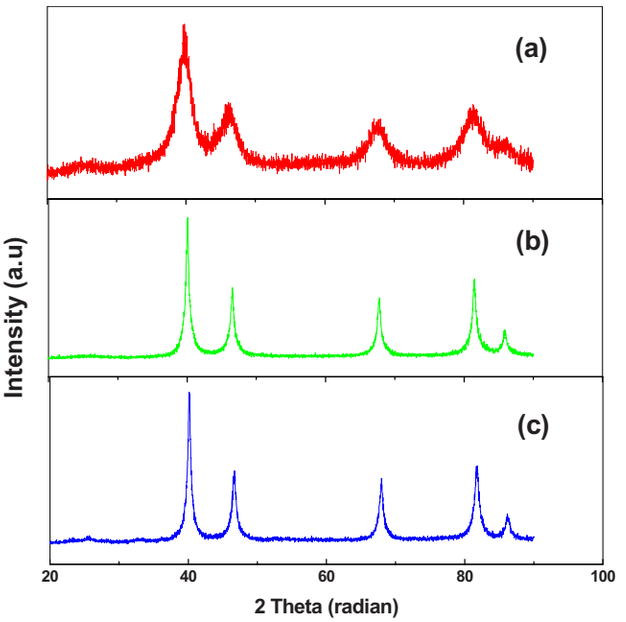

Figure 9. (Color online) Powder XRD patterns for (a) Pt/C, (b) 750 Pt/C, and (c) 750 Pt–TiO_2/C (2:1) catalysts.

XPS is a useful technique to analyze the surface oxidation states in catalyst materials. Accordingly, to gather the information on the oxidation states of Pt in various catalysts, X-ray photoelectron spectra were recorded for the Pt/C, 750 Pt/C, and 750 Pt–TiO_2/C (2:1) catalysts, and the spectra for the Pt (4f) core level region of Pt/C, 750 Pt/C, and 750 Pt–TiO_2/C (2:1) are presented in Fig. 10a-c, respectively. The Pt(4f) regions for Pt/C, 750 Pt/C, and 750 Pt–TiO_2/C (2:1) can be fitted into two sets of spin-orbit doublets. For the Pt/C sample, Pt($4f_{7/2,5/2}$) peaks at 71.09 and 74.39 eV, and 72.1 and 75.17 eV have been assigned to Pt^0 and Pt^{2+}, respectively. For the 750 Pt/C sample, Pt($4f_{7/2,5/2}$) peaks at 71.1 and 74.4 eV, and 72.45 and 75.75 eV are observed for Pt^0 and Pt^{2+}, respectively. The Pt($4f_{7/2,5/2}$) doublets in the 750 Pt–TiO_2/C (2:1) sample at 71.13 and

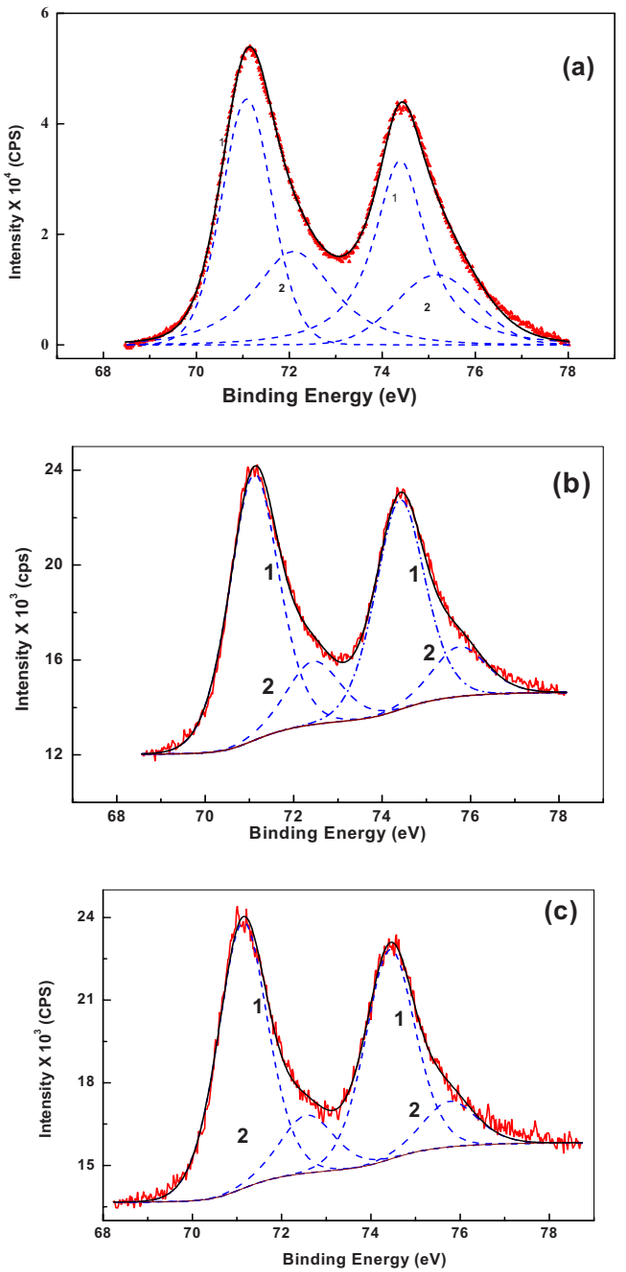

Figure 10. (Color online) X-ray photoelectron spectra for the Pt(4f) region in (a) Pt/C, (b) 750 Pt/C, and (c) 750 Pt–TiO_2/C (2:1). The solid line represents the fitted spectra; 1 and 2 correspond to the Pt^0 and Pt^{2+} species, respectively.

74.43 eV and 72.57 and 75.77 eV have been assigned to Pt^0 and Pt^{2+}, respectively. These data clearly indicate that the Pt binding energy (BE) values for all three samples are nearly similar. The relative intensities for different species are obtained from the respective peak areas. Pt^0 is found to be the predominant species in all the samples, namely, Pt/C, 750 Pt/C, and 750 Pt–TiO_2/C (2:1). The Pt^0 percentage in Pt/C is 60%, while in 750 Pt–TiO_2/C (2:1) it is 77%, a value close to 76% observed for 750 Pt/C. The increase in the Pt^0 percentage of 750 Pt/C and 750 Pt–TiO_2/C (2:1) may be due to the effect of heat-treatment. The BE values and percentages for various species in Pt/C, 750 Pt/C, and 750 Pt–TiO_2/C (2:1) catalysts are presented in Table II.

Table II. BE, fwhm, and relative intensity values for different Pt species as observed from the Pt(4f) spectra for Pt/C, 750 Pt/C, and 750 Pt–TiO_2/C (2:1).

Catalyst	Pt species	BE (eV) $4f_{7/2}$	BE (eV) $4f_{5/2}$	fwhm (eV)	Relative intensity (%)
Pt/C	Pt^0	71.09	74.39	1.33	60
	Pt^{2+}	72.1	75.17	1.83	40
750 Pt/C	Pt^0	71.1	74.4	1.33	76
	Pt^{2+}	72.45	75.75	1.88	24
750 Pt–TiO_2/C (2:1)	Pt^0	71.13	74.43	1.37	77
	Pt^{2+}	72.57	75.77	1.81	23

The alloy formation between Pt and Ti is reported only above 1200°C.[32] Hence, in Pt–TiO_2/C, Ti is expected to be present only in the oxidized state. To examine the exact oxidation state of Ti in 750 Pt–TiO_2/C (2:1), X-ray photoelectron spectrum was recorded for the Ti(2p) region, as shown in Fig. 11. In the spectrum, two peaks are observed at 458.7 and 465 eV, which are attributed to Ti($2p_{3/2}$) and Ti($2p_{1/2}$), respectively. These data confirm the presence of Ti in 750 Pt–TiO_2/C (2:1) as Ti^{4+}. The O(1s) spectra for Pt/C, 750 Pt/C, and 750 Pt–TiO_2/C (2:1) are shown in Fig. 12a and b, respectively. The O(1s) spectrum for Pt/C is not included in the figure because the peak positions (BE values) are nearly similar to that of 750 Pt/C. Three peaks were observed after deconvoluting the O(1s) spectra for both the Pt/C and 750 Pt/C (Fig. 12a). Peak 1 (530.61 eV) is ascribed to O^{2-} in the PtO, peak 2 (532.39 eV) is due to adsorbed OH^- species, and peak 3 (533.82 eV) is due to physisorbed water.[33,34] The O(1s) spectrum for the 750 Pt–TiO_2/C (2:1) catalyst shown in Fig. 12b could be deconvoluted into four components. Peaks 1, 2, and 3 are similar to 750 Pt/C and Pt/C but for the higher intensity for peak 3 in 750 Pt–TiO_2/C (2:1); peak 4 at 529.82 eV is due to O^{2-} in TiO_2. The higher intensity of peak 3 could be due to the hydrated nature of TiO_2.

The surface atomic compositions of the catalysts were also evaluated by EDAX analysis by focusing an electron beam on several different selected regions. The EDAX spectra for the 750 Pt–TiO_2/C catalyst with varying Pt to Ti atomic ratio, namely, 1:1, 2:1, and 3:1, have been obtained, and the compositions at various points on the surface of the samples are close to the nominal values. The EDAX compositions obtained for all the catalysts prepared dur-

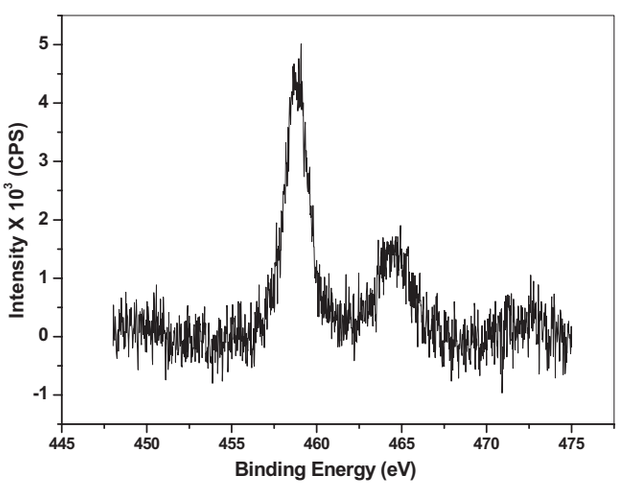

Figure 11. X-ray photoelectron spectrum for the Ti(3p) region in 750 Pt–TiO_2/C (2:1) catalyst.

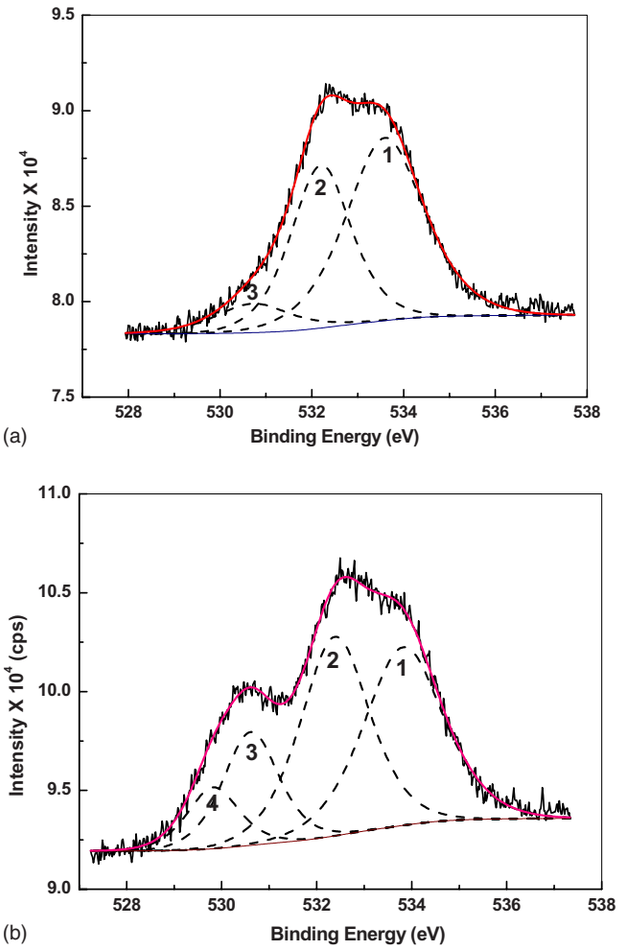

Figure 12. (Color online) X-ray photoelectron spectra for the O(1s) region in (a) 750 Pt/C and (b) 750 Pt–TiO_2/C (2:1). The solid line represents the fitted spectra and the broken line represents the peaks due to various forms of oxides.

ing this study are presented in Table I. The data suggest that, akin to ICP-OES, the surface compositions of the Pt–TiO_2/C catalysts are similar to the bulk.

Conclusions

The incorporation of TiO_2 in carbon-supported Pt ameliorates the electrocatalytic activity of Pt toward oxygen reduction with better methanol tolerance. The DMFC employing a Pt–TiO_2/C heat-treated at 750°C with a Pt to Ti atomic ratio of 2:1 [750 Pt–TiO_2/C (2:1)] exhibits better performance in relation to Pt/C. Powder XRD, TEM, and XPS studies suggest that the dispersion of Pt in the catalyst is improved on the addition of the amorphous titanium oxide.

Acknowledgments

Financial support from CSIR, New Delhi through a suprainstitutional project under EFYP is gratefully acknowledged. G.S is grateful to CSIR, New Delhi for a Senior Research Fellowship.

Central Electrochemical Research Institute assisted in meeting the publication costs of this article.

References

1. J. Larminie and A. Dicks, *Fuel Cell System Explained*, 2nd ed., John Wiley & Sons, England (2003).
2. K. Scott and A. K. Shukla, in *Modern Aspects of Electrochemistry*, R. E. White, C. G. Vayenas, and M. E. Gamboa-Aldeco, Editors, No. 40, p. 127, Springer, New York (2007).
3. E. Antolini, J. R. C. Salgado, and E. R. Gonzalez, *J. Electroanal. Chem.*, **580**, 145 (2005).
4. F. H. B. Lima, W. H. Lizcano-Valbuena, E. Teixeira-Neto, F. C. Nart, E. R. Gonzalez, and E. A. Ticianelli, *Electrochim. Acta*, **52**, 385 (2006).
5. W. Yuan, K. Scott, and H. Cheng, *J. Power Sources*, **163**, 323 (2006).
6. Y. Gong, Y. D. Yeboah, S. N. Lvov, V. Balashov, and Z. Wang, *J. Electrochem. Soc.*, **154**, B560 (2007).
7. E. Antolini, J. R. C. Salgado, A. M. dos Santos, and E. R. Gonzalez, *Electrochem. Solid-State Lett.*, **8**, A226 (2005).
8. P. Hernández-Fernández, S. Rojas, P. Ocón, J. L. Gómez de la Fuente, J. S. Fabián, J. Sanza, M. A. Peña, F. J. Garcìa-Garcìa, P. Terreros, and J. L. G. Fierro, *J. Phys. Chem. C*, **111**, 2913 (2007).
9. J. Mathiyarasu and K. L. N. Phani, *J. Electrochem. Soc.*, **154**, B1100 (2007).
10. H. Li, Q. Xin, W. Li, Z. Zhou, L. Jiang, S. Yang, and G. Sun, *Chem. Commun. (Cambridge)*, **23**, 2776 (2004).
11. M. H. Shao, T. Huang, P. Liu, J. Zhang, K. Sasaki, M. B. Vukmirovic, and R. R. Adzic, *Langmuir*, **22**, 10409 (2006).
12. G. Selvarani, S. Vinod Selvaganesh, S. Krishnamurthy, G. V. M. Kiruthika, P. Sridhar, S. Pitchumani, and A. K. Shukla, *J. Phys. Chem. C*, **113**, 7461 (2009).
13. C. Wang and A. J. Appleby, *J. Electrochem. Soc.*, **150**, A493 (2003).
14. S. R. D'Souza, J. Ma, and C. Wang, *J. Electrochem. Soc.*, **153**, A1795 (2006).
15. G. Selvarani, A. K. Sahu, G. V. M. Kiruthika, P. Sridhar, S. Pitchumani, and A. K. Shukla, *J. Electrochem. Soc.*, **156**, B118 (2009).
16. T. Ioroi, Z. Siroma, N. Fujiwara, S.-I. Yamazaki, and K. Yasuda, *Electrochem. Commun.*, **7**, 183 (2005).
17. J.-M. Chen, L. S. Sarma, C.-H. Chen, M.-Y. Cheng, S.-C. Shih, G.-R. Wang, D.-G. Liu, J.-F. Lee, M.-T. Tang, and B.-J. Hwang, *J. Power Sources*, **159**, 29 (2006).
18. J. Shim, C.-R. Lee, H.-K. Lee, J.-S. Lee, and E. J. Cairns, *J. Power Sources*, **102**, 172 (2001).
19. N. Rajalakshmi, N. Lakshmi, and K. S. Dhathathreyan, *Int. J. Hydrogen Energy*, **33**, 7521 (2008).
20. Y. Fu, Z. D. Wei, S. G. Chen, L. Li, Y. C. Feng, Y. Q. Wang, and M. J. Liao, *J. Power Sources*, **189**, 982 (2009).
21. H.-J. Kim, D.-Y. Kim, H. Han, and Y.-G. Shul, *J. Power Sources*, **159**, 484 (2006).
22. L. Xiong and A. Manthiram, *Electrochim. Acta*, **49**, 4163 (2004).
23. H. Song, X. Qiu, X. Li, F. Li, W. Zhu, and L. Chen, *J. Power Sources*, **170**, 50 (2007).
24. M. Gustavsson, H. Ekstrom, P. Hanarp, L. Eurenius, G. Lindbergh, E. Olsson, and B. Kasemo, *J. Power Sources*, **163**, 671 (2007).
25. L. Brewer and P. R. Wengert, *Metall. Trans.*, **4**, 83 (1973).
26. B. Hammer and J. K. Norskov, *Adv. Catal.*, **45**, 71 (2000).
27. T. L. Barr, *J. Phys. Chem.*, **82**, 1801 (1978).
28. P. Hernández-Fernández, S. Rojas, P. Ocón, A. de Frutos, J. M. Figueroa, P. Terreros, M. A. Peña, and J. L. G. Fierro, *J. Power Sources*, **9**, 177 (2008).
29. W. Jander, *Angew. Chem.*, **42**, 462 (1929).
30. C. Wagner, *J. Phys. Chem. Solids*, **33**, 1051 (1972).
31. G. Crosbie, *J. Solid State Chem.*, **25**, 367 (1978).
32. B. C. Beard and P. N. Ross, *J. Electrochem. Soc.*, **133**, 1839 (1986).
33. C. Jones and E. Sammann, *Carbon*, **28**, 509 (1990).
34. B. Stypula and J. Stoch, *Corros. Sci.*, **36**, 2159 (1994).